

A circular planetary nebula around the OH/IR star OH 354.88–0.54 (V1018 Sco)

Martin Cohen,¹ Quentin A. Parker^{2,3} and Jessica Chapman⁴

¹Radio Astronomy Laboratory, University of California, Berkeley, CA 94720

²Department of Physics, Macquarie University, Sydney, NSW 2109 Australia

³Anglo-Australian Observatory, PO Box 296, Epping, NSW 2121, Australia

⁴Australia Telescope National Facility, PO Box 76, Epping, NSW 2121, Australia

Accepted 2004 November 29. Received 2004 November 29; in original form 2004 March 10

ABSTRACT

New deep, high-resolution H α imagery from the UK Schmidt Telescope (UKST) Unit's H α survey of the Southern Galactic Plane reveals the presence of a faint, highly circular, planetary nebula (PN) surrounding a very long-period variable star (now known as V1018 Sco), first discovered as a 1612-MHz OH maser, OH 354.88–0.54. The nebular phase-lag distance, diameter and radial velocity are 3.2 kpc, 0.3 pc and 13 km s⁻¹, respectively. Combining the maser attributes with near-, mid- and far-infrared data and with our optical spectrum of the ring we conclude that the object was an intermediate-mass asymptotic giant branch (AGB) star (initial stellar mass $\geq 4 M_{\odot}$) in which the fast wind has recently turned on, ionizing previously shed circumstellar material. Hence, we speculate that we may be witnessing a hitherto unobserved phase of PN evolution, in which a PN has only recently started to form around a star that is unequivocally still in its AGB phase.

Key words: masers – stars: AGB and post-AGB – planetary nebulae: general.

1 INTRODUCTION

The source ‘AFGL 5356’ represents the first recognition of anything unusual at $l = 354^{\circ}88$, $b = -0^{\circ}54$ in the form of the discovery of mid-infrared (MIR) emission from a point source in the Revised Air Force Geophysics Laboratory (RAFGL) Rocket Sky Survey of Price & Walker (1976). OH 354.88–0.54 was independently discovered as a strong 1612-MHz maser during a maser survey of the Galactic plane, between $l = 340^{\circ}$ and the Galactic Centre, by Caswell et al. (1981). The 1612-MHz spectrum showed two well-defined peaks with an expansion velocity of ~ 15 km s⁻¹, typical for asymptotic giant branch (AGB) stars with high mass-loss rates. By the early 1980s, OH 354.88–0.54 was recognized to be an extremely heavily obscured star with no detectable optical counterpart. The next 15 yr saw a variety of infrared (IR) measurements of the source, culminating in a secure identification of the object as an extreme, large-amplitude, long-period variable, with several unusual characteristics.

In this paper we bring together the key multiwavelength data on OH 354.88–0.54. We introduce the nebular ring (Section 2), summarize what is currently known about OH 354.88–0.54 from the perspective of the maser (Section 3), the IR photometry (Section 4), and the optical spectrum of the nebula (Section 5), leading to our conclusions about the nature of the nebula (Section 6).

To provide a framework within which to locate the elements of OH 354.88–0.54 described in this paper, we offer the following cross-section of the circumstellar shell of a typical AGB star [Reid

& Menten (1997: their fig. 12), Cohen (1989) and Chapman & Cohen (1986)] by radius and temperature. Stellar photosphere: 3×10^{13} cm, 2400 K; SiO masers: 8×10^{13} cm, 1250 K; dust formation zone: 10^{14} cm, 1100 K; OH 1612-MHz masers: $1 \times 10^{16} - 1 \times 10^{17}$ cm, ~ 50 K.

The unexpected optical detection of the H α ring nebula clearly associated with the OH/IR star has prompted this work because of what it might tell us about the earliest onset of the fast wind in planetary nebula (PN) formation. The overriding issues are to identify the source of ionization for this nebula, to explain its visibility and regular form at a time when the central star is still a long-period variable, and hence locate it in the context of late stellar evolution as it proceeds to the PN phase.

2 DISCOVERY OF THE SURROUNDING H α EMISSION NEBULA

The region of the sky where OH 354.88–0.54 is located shows much complex and diffuse nebular emission. The Anglo-Australian Observatory/United Kingdom Schmidt Telescope (AAO/UKST) H α survey of the Southern Milky Way (Parker & Phillipps 1998, 2003) took a survey exposure of field HA630 (exposure number HA18520) on which a distinct, circularly symmetric nebula (Fig. 1) was discovered. This was during a systematic search for galactic planetary nebulae (PNe) derived from this survey (Parker et al. 2003a). Version 1.0 of the Edinburgh/AAO/Strasbourg Catalogue of Galactic Planetary Nebulae has been released (Parker et al. 2003b), and the

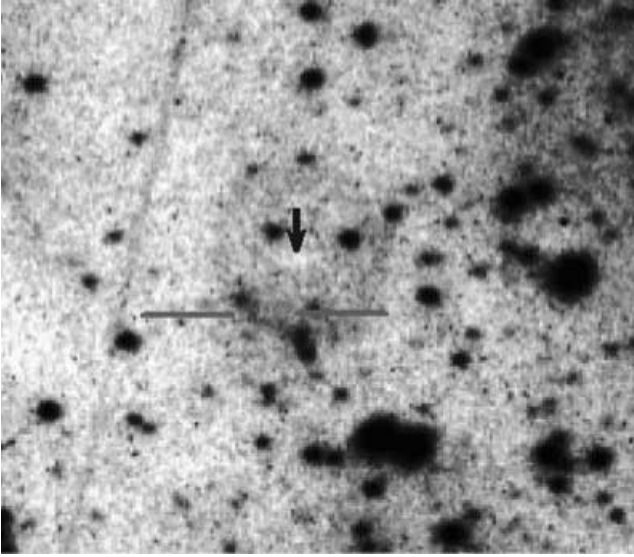


Figure 1. The delicate circular $H\alpha$ ring surrounding the position of OH 354.88–0.54, plotted in Galactic coordinates. The two lines indicate the location of the slit during follow-on spectroscopy (see Section 5). The gap between the lines is to show where we observed the brightest nebulosity around the ring. The optically invisible star lies at the head of the arrow. North is to the top and east to the left. The image size is 128 arcsec in Dec. by 140 arcsec in RA.

effort continues as the Macquarie–AAO–Strasbourg $H\alpha$ PN project (hereafter referred to as the ‘MASH’). The object appears projected against the edge of the highly opaque dark cloud G354.9–00.6 (Hartley et al. 1986), measuring about 4×3 arcmin². The size of the nebula was measured by overlaying circles with a wide variety of centres and radii, from which both the circularity and 39 ± 1 arcsec diameter were determined. As part of the standard procedure for comparing detections of new PN candidates with possible alternative identifications, it was noted that the position of the centroid of the ring (RA $17^{\text{h}}35^{\text{m}}02^{\text{s}}.62 \pm 0.16$, Dec. $-33^{\circ}33'27''.92 \pm 1''.90$, J2000) very closely matched the position of a known strong OH maser source, OH 354.88–0.54. (The positional uncertainties arise from the difficulty in defining the outer edges of the faint ring.) Details of the nebula are given in Table 1, including data presented later in this paper.

Our ongoing multiwavelength studies of new MASH PNe (e.g. Cohen & Parker 2003) includes cross-checking against imagery from the Midcourse Space Experiment (MSX) MIR mission. This led us to recognize a very bright MIR source at the centre of the $H\alpha$ ring. The astrometry of MSX images led to its identification with the known OH maser and with the *IRAS* source, 17317–3331. Note that this star is so bright in the MIR that the brightest pixels create artefacts in the images that result in an atypically poor astrometric position for MSX, some 3.7 arcsec away from the best estimate of the position of the OH/IR star (see Section 3.3).

3 THE MASERS

3.1 OH 1612-MHz spectral characteristics

OH monitoring of OH/IR stars was carried out by several groups during the 1980s (e.g. Herman & Habing 1985; van Langevelde, van der Heiden & van Schooneveld 1990). A long-running programme at the Australian National Telescope Facility (ATNF) of

Table 1. Details of the planetary nebula around OH 354.88–0.54.

MASH	
RA (J2000)	$17^{\text{h}}35^{\text{m}}02^{\text{s}}.62$
Dec (J2000)	$-33^{\circ}33'27''.9$
l, b	$354^{\circ}88, -0^{\circ}54$
Diameter (outer)	39 arcsec
$H\alpha$ survey film	HA18520
$H\alpha$ survey field	630
Date of $H\alpha$ image	1999 August 6
PN designation	PN G354.8–0.5
PHR PN designation	PHR1735–3333
Literature	
AFGL 5356 RA(J2000)	$17^{\text{h}}35^{\text{m}}01^{\text{s}}.8$
AFGL 5356 DEC(J2000)	$-33^{\circ}33'31''$
IRAS 17317–3331 RA(2000)	$17^{\text{h}}35^{\text{m}}02^{\text{s}}.2$
IRAS 17317–3331 DEC(2000)	$-33^{\circ}33'30''$
This work	
Average NIR/MIR RA(2000)	$17^{\text{h}}35^{\text{m}}02^{\text{s}}.72$
Average NIR/MIR DEC(2000)	$-33^{\circ}33'29''.40$
Average OH maser RA(2000)	$17^{\text{h}}35^{\text{m}}02^{\text{s}}.73$
Average OH maser DEC(2000)	$-33^{\circ}33'29''.41$
Distance	3.2 kpc
Diameter	0.3 pc
Radial velocity (LSR)	-10 km s^{-1}
Density	4000 cm^{-3}
Stellar velocity (LSR)	9.4 km s^{-1}
Ionized gas mass	$0.35 M_{\odot}$
Filling factor	0.02

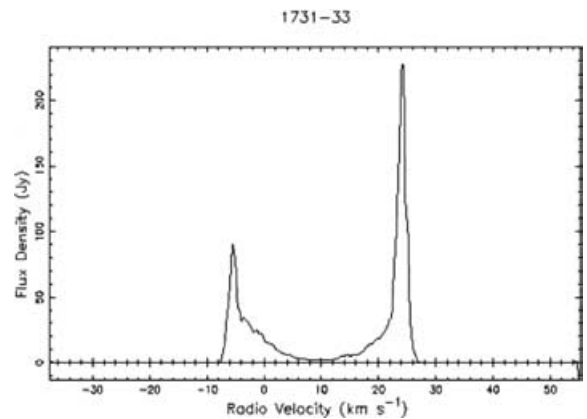


Figure 2. The average 1612-MHz spectral profile of OH 354.88–0.54 from 36 separate epochs of observation at Parkes. Note the non-zero flux level at the centre of the profile, near the stellar velocity. All velocities are reduced to LSR values.

monitoring OH/IR masers associated with *IRAS* sources, by Chapman and colleagues, observed OH 354.88–0.54 using Parkes at 1612 MHz during 36 epochs between 1988 December and 1993 July. It is seen to have the classic double-peaked spectrum of a strong OH/IR star, but its strength is such that emission is detected across the stellar velocity, rather than falling to zero, as is more typical of this class of maser. Fig. 2 presents the averaged profile from these 36 data sets; these data have never been previously published. The blueshifted peak velocity is -5.5 km s^{-1} and the redshifted peak velocity is $+24.3 \text{ km s}^{-1}$. These indicate that the systemic velocity of the star is $+9.4 \text{ km s}^{-1}$ (local standard of rest, hereafter ‘LSR’)

and the shell is expanding at 14.9 km s^{-1} , where each velocity is measured to a precision of 0.18 km s^{-1} . This systemic velocity does not correspond to a plausible distance for the star based on Galactic rotation (24 kpc), indicative of a peculiar velocity.

Frail & Beasley (1994) sought OH/IR stars in a sample of globular clusters, noting the proximity in the sky of OH 354.88-0.5 to the cluster, Liller 1. They rejected any association with the cluster on the basis of radial velocity. Sevenster et al. (1997a) reobserved the maser during a systematic survey for sources of OH 1612 MHz maser emission in the Galactic plane and bulge in late 1993. The spectral profile derived from her data is entirely consistent with that in Fig. 2, although the flux densities of both peaks are lower than in our data because Sevenster et al. observed near IR minimum light. The last 1612-MHz observation of which we are aware was taken on 1999 November 11 at the Australia Telescope Compact Array (ATCA) while setting up for an OH observing run. The spectral profile indicates that the OH emission character of OH 354.88–0.54 had not changed at a time only a few months after the $\text{H}\alpha$ exposure was taken.

3.2 Light curve, stellar period and phase lag

The light curve for the maser (expressed as the average of the front and back peaks), corresponding to the data averaged in Fig. 2, is shown in Fig. 3, from which the 1612-MHz period is determined to be $1486 \pm 20 \text{ d}$ (Chapman, Habing & Killeen 1995). The associated best-fitting curve also appears in this figure, on the basis of a simple combination of the fundamental period and a single harmonic.

The linear size of a circumstellar envelope can be determined by measuring the phase lag, or time-delay between the arrival times of maser emission from the front and back of the circumstellar envelope. For OH 354.88–0.54, the measured phase lag is one of the largest known among the 95 sources monitored at Parkes. The best-fitting value has been determined by separately fitting a 1486-d period to blue and red peaks to assess the arrival time of maxima. The lag is $60 \pm 9 \text{ d}$, and corresponds to a linear diameter of $1.6 \times 10^{17} \text{ cm}$ (11 000 au), making this an unusually large shell. The lag can readily be seen in Fig. 4, which represents the first appearance of these data and their fits. While this is not the largest phase lag known for such a maser, one can gain a sense of just how rare such large phase lags are from the analysis by van Langevelde et al.

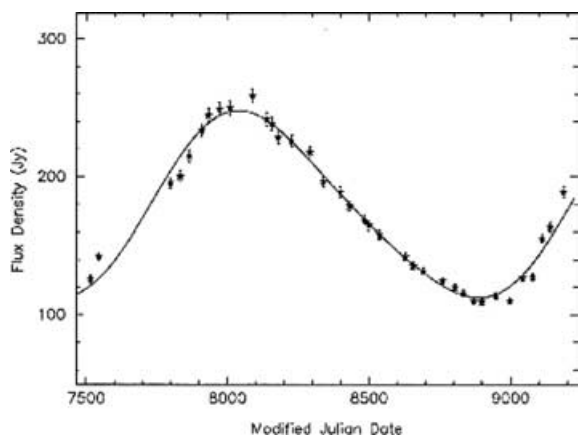


Figure 3. The 1612-MHz light curve of OH 354.88–0.54 assembled from the 36 epochs of Parkes’ data, from a weighted average of the emission across the blueshifted and redshifted peaks. The best-fitting curve for a period of 1486 d is shown fitted to these data. Dates are JD expressed as $2440000 +$ the abscissa.

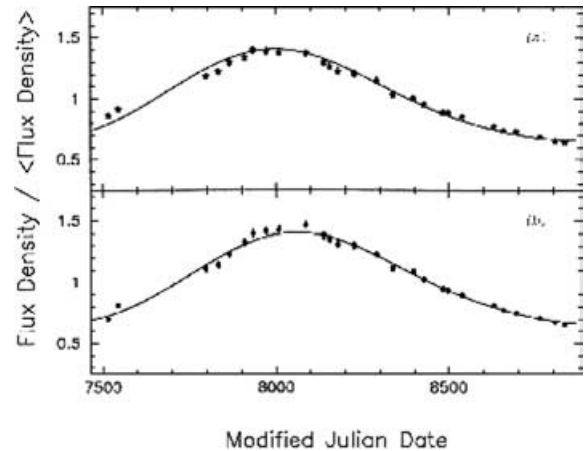


Figure 4. Light curves for the OH 1612-MHz blueshifted (a; top) and redshifted (b; bottom) emission peaks of OH 354.88–0.54, corresponding to velocities of -5.5 and $+24.3 \text{ km s}^{-1}$, respectively. In each case, the peak flux densities are normalized by the mean flux density. The phase lag between the front and back of the circumstellar envelope is clearly evident. Each curve is shown using our best-fitting period.

(1990) of a sample of 1612-MHz masers monitored at Dwingeloo. Of 43 masers with definite OH variability, only three have significantly detected lags that exceed the 60 d of OH 354.88–0.54, and all three have very long periods comparable to or greater than that of OH 354.88–0.54.

3.3 Maser position refinement

Five independent sets of OH maser positions are available. It is important to establish that these represent the same object – the long-period variable – rather than a set of ‘hot spots’ that appear and disappear over time like those associated with cool supergiant sources such as VY CMa. These maser positions are due to: Bowers & Knapp (1989) with the Very Large Array (VLA) in A/B-configuration at 1612 MHz; Becker, White & Proctor (1992) with the VLA in B-array at 1612 MHz; Fix & Mutel (1984) with the VLA in A-configuration at 1612 MHz; Sevenster et al. (1997a,b) with ATCA at 1612 MHz; and Caswell (1998), through high signal-to-noise observations of the associated 1665/1667-MHz emission. The ratio of peak emissions of the maser at 1665 : 1667 : 1612 MHz is roughly 1 : 4 : 400, and these are typical ratios for OH/IR stars. The VLA has a significantly smaller beam size than the ATCA at 1612 MHz, but the ATCA positions have smaller formal uncertainties so we are inclined simply to average all five positions with equal weights. This yields a best estimate for the position of the star itself as: RA $17^{\text{h}}35^{\text{m}}02^{\text{s}}.73 \pm 0^{\text{s}}.02$, Dec. $-33^{\circ}33'29''.41 \pm 0''.24$. Therefore, the estimated centre of the $\text{H}\alpha$ ring lies within 1σ of the stellar position.

3.4 OH 1612 MHz maser distribution and stellar distance

Welty, Fix & Mutel (1987) published well-resolved, VLA, A-array images of the OH 1612-MHz shell of OH354.88–0.54. The emission was clearly strongest in an east–west (E–W) plane and weaker to the north (N) and south (S). We interpret this as a well-filled torus around the star with less dense emission along a polar axis. From their maps near the stellar velocity we estimate the angular diameter to be $3.3 \pm 0.3 \text{ arcsec}$, measured from the separation of the prominent pair of emission knots.

Combining the phase lag diameter of 1.6×10^{17} cm with this angular diameter yields a distance of 3.2 kpc. The likely uncertainty on this distance estimate is about 20 per cent from the combination in quadrature of a 15 per cent error in phase lag and 15 per cent in angular diameter. While the phase lag method must yield the most accurate distance estimate, it is noteworthy that Le Sidaner & Le Bertre (1996) cite a period–luminosity distance of 3.5 kpc, although they finally adopted 3 kpc in their modelling of this star.

3.5 Other masers in OH 354.88–0.54

86-GHz SiO maser emission is very weak in this star, but definitely present. Nyman, Hall & Le Bertre (1993) found unusual SiO properties for OH 354.88–0.54 with a ratio of integrated 43-GHz ($v = 1, J = 1 \rightarrow 0$) to 86-GHz ($v = 1, J = 2 \rightarrow 1$) emission >18 , and a very high ratio of the $J=1 \rightarrow 0$ $v = 2/v = 1$ transitions at 43 GHz of 4.4. The average 43/86-GHz line strength ratio is only 0.42 in Miras and supergiants (Lane 1982), while the 43-GHz line ratio is ~ 1 in Miras, supergiants and semi-regular variables (e.g. Lane 1982) and ~ 2 in warmer OH/IR stars (Nyman et al. 1993). In their survey of 313 inner Galaxy *IRAS* sources with the colours of late-type stars, Jiang et al. (1995) found no object with an integrated 43-GHz line ratio greater than 4. Nakashima & Deguchi (2003) remeasured the 43-GHz SiO maser lines in OH 354.88–0.54, finding a ratio of 3.7, less extreme than that of Nyman et al. (1993). Nakashima & Deguchi (2003) also present a valuable diagram correlating this line ratio in many *IRAS*-selected masers with [12–25] colour index. From this diagram one can see that OH 354.88–0.54 is by no means unique in terms of this line ratio; 7 per cent of the sample of 143 masers have ratios above 4.

3.6 The nature of OH 354.88–0.54

The OH 1612-Hz maser data are characteristic of maser emission from an OH/IR star with a high expansion velocity (~ 15 km s^{-1}), an exceptionally long pulsation period (1500 d), and an extremely large OH shell (1.6×10^{17} cm). The large-amplitude pulsations evident in the OH light curves indicate that the star is still pulsating strongly, and has not yet left the AGB stage of evolution, while the large masing envelope size and high expansion velocity indicate a fairly high mass star with an initial stellar mass of $\geq 4 M_{\odot}$ (and probably more: see Chapman et al. 1995). Neither irregular nor bipolar outflows are inferred from the OH maser spectral profile or spatial distribution.

4 INFRARED OBSERVATIONS

4.1 Near-IR measurements

Jones et al. (1982) sought the IR counterpart of OH 354.88–0.54 in L' , while Epchtein & Nguyen-Quang-Rieu (1982) searched in K . This difference in strategy most likely accounts for the discrepancies of 4^m in K and L' between the contemporaneous photometry from these two groups. The real source was very faint in K during early 1981, and probably undetected by Epchtein et al., causing them to identify a different object which they characterized as a probable reddened field star rather than the true IR counterpart of OH 354.88–0.54. Le Bertre (1988) estimated its period from near-infrared (NIR) monitoring to be >1200 d. Le Bertre & Nyman (1990) reported OH 354.88–0.54 to be one of the reddest known OH/IR objects, with a $K - L$ colour index >6 . Long-term IR monitoring at 15 epochs between 1986 March and 1990 July in the L' and M bands enabled Le Bertre (1993) to derive periods of 1418

(L') and 1448 d (M). The average of these IR periods, 1433 d, was cited by Nyman et al. (1993), and is consistent with our OH-based period at the 1σ level. This long period and large amplitude are entirely in keeping with the NIR redness and faintness at J , below 16th magnitude when observed by 2MASS (on JD2451039 in 1998 August, at phase 0.14, close to the expected epoch of another IR minimum). Inspection of the 2MASS trio of images corroborates the J and H invisibility of the star, even at levels well below those of the 2MASS point source archive, but readily reveals the object in the K band. The minimum amplitudes of NIR variability, based on combining 2MASS data with those in the literature, are: $\Delta J \sim 4.9$, $\Delta H \sim 5.4$, $\Delta K \sim 3.4$, $\Delta L' \sim 6.9$ and $\Delta M \sim 6.3$. OH 354.88–0.54 is indeed an extreme variable.

4.2 MIR measurements

The MIR emission of OH 354.88–0.54 was first measured at 4, 11 and 20 μm (Price & Walker 1976). *IRAS* subsequently detected broad-band emission at 12, 25, and 60 μm . OH 354.88–0.54 was imaged using the IR speckle technique at 10 μm by Cobb & Fix (1987) who drew attention to the unusual degree of asymmetry between its measured N–S and E–W diameters [0.37 ± 0.015 arcsec, 0.23 ± 0.025 arcsec, with the ratio of N–S/E–W of 1.63 ± 0.19]. At the distance of 3.2 kpc, these translate into physical dimensions of 1.8×10^{16} (N–S) and 1.1×10^{16} cm (E–W), roughly a factor of 10 smaller than the E–W extent of the 1612-MHz distribution.

We have extracted three individual *IRAS* spectra of this source from the Low Resolution Spectrometer (LRS) data base and have corrected their shapes and recalibrated them as described by Cohen et al. (1992a) and Cohen, Walker & Witteborn (1992b), using the contemporaneous 12- μm measurements from the *IRAS* Working Survey Data Base (WSDB). Fig. 5 illustrates these time-resolved spectra. Circumstellar silicate absorption features show deeply at 10 μm , with the associated broad, shallow absorptions centred near 18 μm . The time-separations between the two (almost coincident) upper LRS spectra, and between the second and the third spectrum were 7 and 166 d, respectively, spanning a total interval of 0.11 in light-curve phase. The optical depths in the 10- μm silicate feature

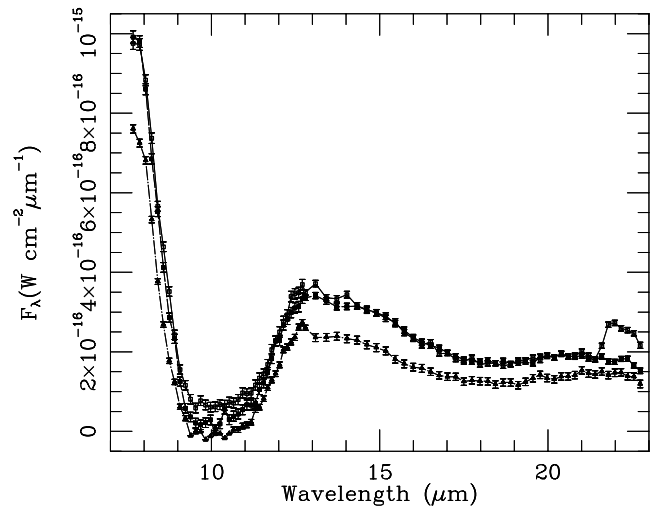


Figure 5. The three independent *IRAS* LRS spectra of OH 354.88–0.54 from different phases of the MIR light curve. 1σ error bars are shown on all points. The apparent feature near 22 μm in the upper spectrum is caused by an electronic glitch in the baseline of the red spectrometer during that particular spectrum.

(τ_{10}) were 2.3, 3.0 and 4.0, respectively, and are somewhat dependent on the interpolated continua. This shows the pattern of increasing τ_{10} as the star declines toward minimum light as predicted by Le Berre (1993) for AGB stars with very thick dust shells. These values suggest a total line-of-sight extinction of $A_V \sim 40\text{--}80$ mag.

Le Sidaner & Le Berre (1996; their table 4, final column) attribute 1.7 mag at 10 μm to the purely interstellar extinction toward this star. Using the plots of $E(B - V)$ with distance by Fitzgerald (1968) and Lucke (1978) we estimate from our phase-lag distance that the star must suffer an A_V from 1–3.5 mag. Therefore, the circumstellar reddening dominates the interstellar component.

These LRS spectra are very typical of the most extremely red O-rich LPVs (see Fig. 2a of Wainscoat et al. 1992). The star has been modelled by Suh (1999: using the mean LRS spectrum), who adopts $\tau_{10} = 20$, a stellar temperature of 2000 K and luminosity of $10^4 L_\odot$, and a dust opacity function specific to cool silicate grains to fit both silicate absorption features. Le Sidaner & Le Berre (1996: using IR photometry) use 1800 K, $1.7 \times 10^4 L_\odot$ and $\tau_{10} = 11.2$. They derive a substantial dust mass-loss rate of $7 \times 10^{-7} M_\odot \text{yr}^{-1}$. Using their value of 100 for the circumstellar gas-to-dust ratio, this gives a total mass loss rate of $7 \times 10^{-5} M_\odot \text{yr}^{-1}$, consistent with a star of at least intermediate mass. Chen et al. (2001) argue from their analysis of 1024 OH maser sources with LRS spectra that those with silicate absorption represent a higher mass population than the more frequently encountered AGB stars with silicate emission.

The MSX Galactic plane survey and its Point Source Catalog (PSC1.2) show a very bright MIR source (Table 2) at the location of the OH maser. Using the embedded 2–35 μm spectral library from the SKY model of the point source sky (Cohen 1994) we have synthesized the colours of all 87 categories of IR source in SKY from the relative response curves for the MSX bands. On the basis of comparison with these 87 classes of object we determine that OH 354.88–0.54 is a star that is slightly more extreme than the reddest O-rich AGB star of type M (O-rich) (AGBM) stars represented in the SKY model.

4.3 The IR position of the star

The weighted average location of the combination of 2MASS K , Jones et al. (1982) L' , *IRAS* and MSX positions is RA $17^{\text{h}}35^{\text{m}}02^{\text{s}}.72 \pm 0^{\text{s}}.13$, $-33^{\circ}33'29''.40 \pm 1''.83$, which is in excellent agreement (well within 1σ) with the accurate OH position for the star and with the estimated centre of the H α ring.

Table 2. Median NIR and Mean MIR/FIR Photometry from the Literature of OH 354.88–0.54.

Waveband	Mag/Flux Density
<i>J</i>	14.3 mag
<i>H</i>	12.4 mag
<i>K</i>	11.6 mag
<i>L'</i>	3.5 mag
<i>M</i>	1.1 mag
MSX <i>F</i> (4 μm) (Jy)	13.1 ± 1.5
MSX <i>F</i> (8 μm) (Jy)	70.8 ± 3.5
MSX <i>F</i> (12 μm) (Jy)	100.1 ± 3.0
MSX <i>F</i> (15 μm) (Jy)	168.2 ± 6.7
MSX <i>F</i> (21 μm) (Jy)	221.0 ± 13.3
<i>IRAS F</i> (12 μm) (Jy)	104.0
<i>IRAS F</i> (25 μm) (Jy)	291.5
<i>IRAS F</i> (60 μm) (Jy)	234.5
<i>IRAS F</i> (100 μm) (Jy)	<736

4.4 Mid- and far-IR colour–colour planes

On the basis of its *IRAS* colours, OH 354.88–0.54 was variously described as a young stellar object (of T Tauri type) in a dark cloud (Persi et al. 1990), a young PN (Zijlstra et al. 1989), and was re-discovered as an *IRAS* source having the colours of a PN in the 12–25/25–60 μm plane by Garcia-Lario et al. (1997), who also made NIR photometric measurements between 1 and 5 μm . This varied character arises because these colour–colour boxes or ‘occupation zones’ often overlap (Walker & Cohen 1988; Walker et al. 1989), despite the convenience of representing colour–colour planes as having distinct compartments (van der Veen & Habing 1988).

The *IRAS* [12–25],[25–60] colour–colour plane has been widely utilized over the past two decades as a tool for diagnosing the nature of *IRAS* sources (e.g. Walker & Cohen 1988; van der Veen & Habing 1988). Its specific application to OH/IR stars has been pursued most recently by Sevenster et al. (1997a,b) and Sevenster (2002a,b) using colours $[12\text{--}25] = 2.5 \log_{10} F_\nu(25)/F_\nu(12)$ and $[25\text{--}60] = 2.5 \log_{10} F_\nu(60)/F_\nu(25)$. All flux densities are measured in Jy. Sevenster’s *IRAS* colours, like her MSX colours, follow the convention that excludes the zero-point constants, offsetting her planes from any absolutely-defined versions of these. To avoid confusion we offer only diagrams based on this popular convention in this paper.

Sevenster (2002b) has explored the separation between AGB and post-AGB stars, dividing OH/IR stars into ‘RI’ and ‘LI’ groups. The distinction between these two groups is intended to be whether their location in this *IRAS* colour–colour diagram is to the left (LI) or right (RI) of the evolutionary sequence first defined in this plane by van der Veen & Habing (1988). Miras and OH/IR stars are located on or very near this evolutionary track. Most well-studied post-AGB stars are in the RI region. This is the traditional region for finding post-AGB stars, and Sevenster (2002b) has argued that these are lower-mass stars ($\sim 2 M_\odot$) that will become elliptical/circular PNe. The LI region, discussed extensively only by Sevenster (2002a,b), is associated with intermediate-mass AGB stars ($\geq 4 M_\odot$) which Sevenster speculates are more likely to become bipolar PNe. This is also in accord with the much lower mean Galactic latitude of the LI sources (0.46°) compared with that for RI sources (1.66°). The average shell expansion velocities of OH/IR stars in the RI group are below 15 km s $^{-1}$, while those of the LI group are above (Sevenster 2002a,b).

Fig. 6 is an adaptation of Sevenster’s *IRAS* colour–colour plane showing likely AGB and post-AGB stars currently under investigation at ATNF (R. Deacon, private communication). Deacon’s sample of 85 stars includes some objects chosen by their *IRAS* colours, and others by their MSX colours. We calculated the three individual sets of *IRAS* colours from the WSDb time-resolved measurements of OH 354.88–0.54 and plotted them in Fig. 6. Within the photometric uncertainties, all three locations, corresponding to IR light-curve phases 0.57–0.69 during the *IRAS* mission, lie along the evolutionary track of van der Veen & Habing (1988), moving monotonically up the track with time (large crosses). The *IRAS* colours of OH 354.88–0.54 place it near the lower right-hand corner of the LI zone, and its expansion speed of 14.9 km s $^{-1}$ also suggests its proper association with the LI sources. Fig. 7 is likewise an adaptation of Sevenster’s suggested MSX colour–colour plane for distinguishing LI from RI sources. OH 354.88–0.54 lies with the LI sources. Table 2 summarizes median or mean IR photometry for OH 354.88–0.54. The resulting bolometric luminosity from this table is $3.1 \times 10^4 L_\odot$. Therefore, all this object’s MIR attributes are consistent with a somewhat massive and still pulsating variable with the properties of the LI stars.

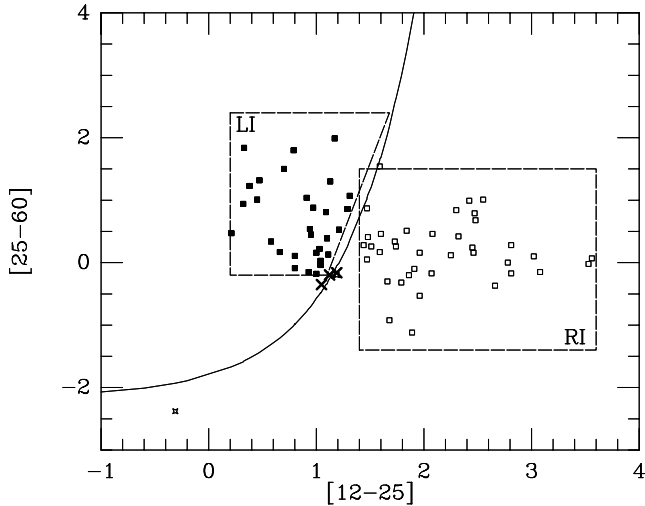


Figure 6. *IRAS* colour–colour plane showing an attempt to separate OH maser sources into LI and RI zones (the dashed boxes), and comparing these with the suggested evolutionary sequence of van der Veen & Habing (1988). The three independent *IRAS* observations of OH 354.88–0.54 are represented by the set of three large crosses along this sequence near the lower right-hand corner of the LI zone, moving in time up and to the right along the track. The symbols denote LI (filled squares) and RI (open squares) stars.

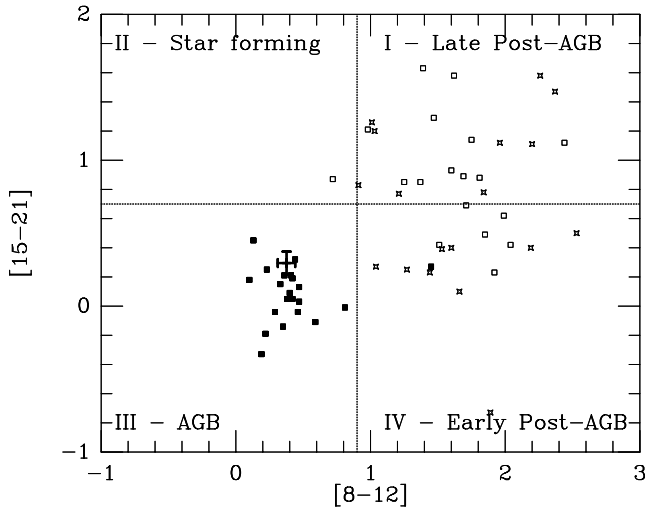


Figure 7. Sevenster's suggested four-quadrant MSX colour–colour diagram in which quadrants III and I/IV respectively separate OH masers into LI (filled squares) and RI objects (open squares). OH 354.88–0.54 is the large cross among the LI sources, showing its 1σ uncertainties in the MSX colours. Open star symbols represent sources not yet definitively assigned to RI status.

5 THE OPTICAL SPECTRUM OF THE NEBULAR RING

During the programme of spectroscopic follow-up of MASH PNe candidates on the South African Astronomical Observatory (SAAO) 1.9-m telescope, a long-slit (2 arcmin) spectrum of the newly identified $H\alpha$ ring (within which the maser source is centred) was taken on 2003 June 28 (JD2452819, phase 0.30). The instrumental configuration was similar to that described by Parker &

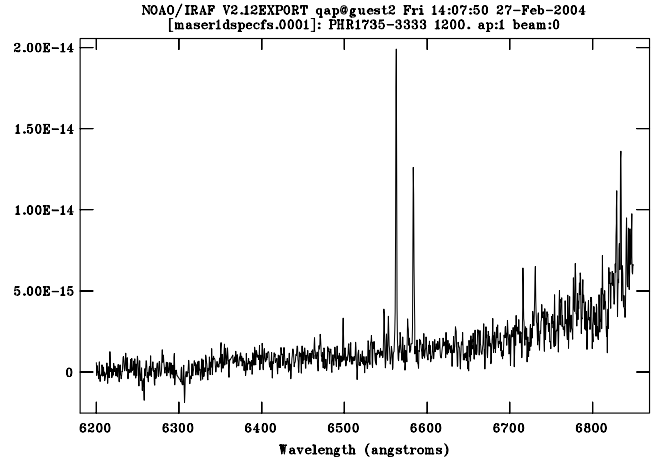


Figure 8. The emission-line spectrum of the $H\alpha$ ring around OH 354.88 – 0.54.

Morgan (2003) with the use of a high dispersion 1200R grating, giving $\sim 0.4 \text{ \AA pixel}^{-1}$ over the range 6152–6912 \AA . Wavelength calibration was via Copper–Argon arc lamp exposures taken on either side of the 1200-s exposure on the $H\alpha$ ring. The location of the slit is indicated in Fig. 1. A nebular detection was obtained confirming the veracity of the optical shell. The nebula spectrum was flux-calibrated using the spectrophotometric standard star LTT6248 taken 15 min prior to the target exposure. The spectrum is given in Fig. 8, which shows $H\alpha$ /[N II] and [S II] emission lines together with evidence of a faint red continuum. The abruptly rising red continuum we attribute to contamination by a faint red star within the slit. Consequently, we regard the spectrum as that of a planetary nebula, because it is circularly symmetric, centred on an evolved exciting star of intermediate mass, still a red AGB star, and exhibits the canonical emission lines associated with such nebulae.

The weighted average of the heliocentric radial velocities of these five lines is $-13 \pm 5 \text{ km s}^{-1}$, equivalent to an LSR velocity of $-10 \pm 5 \text{ km s}^{-1}$. The ratio of the sulphur lines, $I(6717)/I(6731)$, is 0.59. Adopting $T_e = 10^4 \text{ K}$, and using table 5.7 of Osterbrock (1989) yields $N_e \sim 4000 \text{ cm}^{-3}$.

One can estimate the ionized gas mass (M_i) in the PN from the correlation for Galactic disc PNe between M_i and absolute size derived by Boffi & Stanghellini (1994: their equation 9). We find $M_i = 0.35 M_\odot$. Using the expression for M_i in a PN given by Boffi & Stanghellini (1994) in their equation (5), treating the PN as a sphere of radius $\sim 10^{18} \text{ cm}$ ($\sim 20 \text{ arcsec}$ at 3.2 kpc), with N_e determined from the red [S II] lines, the deduced filling factor is 0.02. Thus this PN is characterized by a somewhat larger than average ionized mass and a smaller than average filling factor.

6 CONCLUSIONS

We have identified a faint, circular nebula with a typical PN spectrum, centred on an extremely red, long-period variable star associated with a bright OH 1612-MHz maser. The PN spectrum is proof of the reality and nature of the $H\alpha$ nebula, and the good centring of the OH maser suggests a causal link between the long-period variable and the nebula. The $H\alpha$ survey image covered the position of the OH/IR star on JD2451338 (1999 August 6) at a light-curve phase of the IR variation of the star of 0.34, almost the same as the phase at which the optical spectrum was obtained (0.30). The optical spectrum of the nebula samples the expanding gas only near the

tangent to the ring, giving us rather limited information on the outflow velocity of the gas far from the star. The formal difference between the systemic velocity of the star and that of the nebular emission lines is $\sim 20 \text{ km s}^{-1}$, but this must be a lower bound on the true outflow speed because of our viewing geometry at the edge of the ring. Could it be fast enough to collisionally ionize the ambient gas? The spectrum reveals no hint of [O I] 6300/6363 Å emission lines, but our wavelength region did not cover [O II] 7320/7330 Å nor He I 5876 Å, lines that could signify gas cooling after a shock at a velocity between a few tens and $\sim 100 \text{ km s}^{-1}$. At much lower velocities, the resulting fractional ionization of H would be too low for us to detect. If the nebular emission were due solely to shock interaction with the surrounding interstellar medium (ISM), one would not expect a uniformly bright nebula, because the interaction would produce emission line cooling strongly dependent on local density inhomogeneities encountered in the ISM. We plan to reobserve this nebula with a larger telescope, to widen our wavelength coverage, and to secure new nebular spectra at several light curve phases.

The central star appears to come from a progenitor of intermediate mass ($\geq 4 M_{\odot}$). It is still pulsating strongly, and moving along a suggested evolutionary track characteristic of Miras and OH/IR stars. If OH 354.88–0.54 were truly an LI source, Sevenster has argued that such objects are more likely to become bipolar PNe. The high signal-to-noise ratio OH spectral profile we present shows no hint of bipolarity as yet, based upon the OH profiles predicted by Zijlstra et al. (2001) that signal the onset of bipolarity in early post-AGB stars. The OH envelope around this star is elongated in an E–W direction but sparser in maser emission at its poles (N–S), like an edge-on torus. MIR stellar emission is elongated orthogonal to the OH maser emission, suggesting that any outflowing gas in which dust grains have condensed is dominantly in the polar directions. Therefore, the MIR emission is likely to represent a more recent phenomenon than the accumulated toroid of OH gas. Might this signify the earliest onset of the fast wind (Kwok, Purton & Fitzgerald 1978) in this source?

The existence of the ionized nebula poses the question of what mechanism for ionization such an AGB star has available to it. The OH spectral profile indicates no evidence for a hot binary companion, precluding direct radiative ionization of the circumstellar gas. OH envelopes around long-period variables are known to be sparsely populated and dominated by a relatively small number of clumps (Welty et al. 1987; van Langevelde et al. 1990). Therefore, conceptually, a fast wind might penetrate through the toroid containing the OH molecules and far into the circumstellar region, producing collisional ionization of the accumulated material previously shed by the star during its AGB evolution.

One other scenario is worth considering as a possible source of nebular ionization. If the central AGB star were a ‘born-again’ (e.g. Iben 1984) object that had undergone a ‘very late thermal pulse’ (‘VLTP’; e.g. Blöcker & Schönberner 1997) as it entered the cooling track, then material would have been shed and ionized by the hot central star as it created a PN at the end of its former AGB life. Given sufficient remaining core helium, this late helium flash would have returned the central star to the AGB within a very short period of time (a few hundred years in a star initially of roughly solar mass and abundances: Lawlor & MacDonald 2003, their table 2). Perhaps the currently OH-masing, long-period IR variable never had to ionize the nebulous ring. Empirical estimates for the luminosity of the star range from 1.7×10^4 (Le Sidaner & Le Bertre 1996) to $3.1 \times 10^4 L_{\odot}$ (Table 2), implying a bolometric magnitude between -5.85 and -6.50 , respectively. Vassiliadis & Wood (1993) have modelled the evolution of AGB stars. From their table 2, one derives

a minimum initial mass for the progenitor of OH 354.88–0.54 of $4\text{--}5 M_{\odot}$ and an expected core mass of $\sim 0.8\text{--}0.9 M_{\odot}$. This initial mass is higher than those of the roughly solar-mass stars undergoing VLTPs discussed by Lawlor & MacDonald (2003), and Vassiliadis & Wood (1994) did not incorporate VLTPs into their work on the evolution of intermediate-mass stars. If a $4\text{--}5 M_{\odot}$ progenitor could undergo the VLTP phenomenon, is it likely that the PN ejected after the first AGB phase of evolution would have remained ionized while the star rejoined the AGB? The recombination time-scale for the PN around OH 354.88–0.54, with $T_e = 10^4$, would be $\approx 10^5/N_e$ yr (e.g. Marten & Szczerba 1997) or 25 yr. It would be remarkable if such a progenitor could accomplish its post-VLTP evolution and return to the AGB within only a few years. It is also noteworthy that this star has shown no hint of the rapid changes of behaviour so characteristic of other possible VLTP sources such as V605 Aql and FG Sge.

Therefore, we speculate that we may be witnessing a hitherto unobserved phase of PN evolution, in which a PN has only recently started to appear around a star that is unequivocally still in its AGB phase.

ACKNOWLEDGMENTS

MC thanks NASA for supporting this work under its Long Term Space Astrophysics and Astrophysics Data Analysis programmes, through grants NAG5-7936 and NNG04GD43G with UC Berkeley. The AAO has undertaken the H α survey on behalf of the astronomical community. We thank Jim Caswell for his ever reliable and well-documented dossier on the early OH survey; Nicolas Epchtein and Terry Jones for helping us to understand the discordant NIR measurements from February 1981; Rachel Deacon for providing us with a table of the IRAS and MSX flux densities for her samples of maser sources; and Falk Herwig for valuable discussions about the VLTP phenomenon in AGB stars.

REFERENCES

- Becker R. H., White R. L., Proctor D. D., 1992, *AJ*, 103, 544
 Blöcker T., Schönberner D., 1997, *A&A*, 324, 991
 Boffi F. R., Stanghellini L., 1994, *A&A*, 284, 248
 Bowers R. F., Knapp G. R., 1989, *ApJ*, 347, 325
 Caswell J. L., 1998, *MNRAS*, 297, 215
 Caswell J. L., Haynes R. F., Goss W. M., Mebold U., 1981, *Aust. J. Phys.*, 34, 333
 Chapman J. M., Cohen R. J., 1986, *MNRAS*, 220, 513
 Chapman J. M., Habing H. J., Killeen N. E. B., 1995, in Stobie R. S., Whitelock P. A., eds, *ASP Conf. Ser. Vol. 83, Astrophysical Applications of Stellar Pulsations*. Astron. Soc. Pac., San Francisco, p. 113
 Chen P. S., Szczerba R., Kwok S., Volk K., 2001, *A&A*, 368, 1006
 Cobb M. L., Fix J. D., 1987, *ApJ*, 315, 325
 Cohen R. J., 1989, *Rep. Prog. Phys.*, 52, 881
 Cohen M., 1994, *AJ*, 107, 582
 Cohen M., Parker Q. A., 2003, in Dopita M., Kwok S., Sutherland R., eds, *Proc. IAU Symp. 209, Planetary Nebulae and Their Role in the Universe*. Astron. Soc. Pac., San Francisco, p. 33
 Cohen M., Walker R. G., Barlow M. J., Deacon J. R., 1992a, *AJ*, 104, 1650
 Cohen M., Walker R. G., Witteborn F. C., 1992b, *AJ*, 104, 2030
 Epchtein N., Nguyen-Quang-Rieu, 1982, *A&A*, 107, 229
 Fitzgerald M. P., 1968, *AJ*, 73, 983
 Fix J. D., Mutel R. L., 1984, *AJ*, 89, 406
 Frail D. A., Beasley A. J., 1994, *A&A*, 290, 796
 García-Lario P., Manchado A., Pych W., Pottasch S. R., 1997, *A&AS*, 126, 479

- Hartley M., Tritton S. B., Manchester R. N., Smith R. M., Goss W. M., 1986, *A&AS*, 63, 27
- Herman J., Habing H. J., 1985, *A&AS*, 59, 523
- Iben I., 1984, *ApJ*, 277, 333
- Jiang B. W., Deguchi S., Izumiura H., Nakada Y., Yamamura I., 1995, *PASJ*, 47, 815
- Jones T. J., Hyland A. R., Gatley I., Caswell J. L., 1982, *ApJ*, 253, 208
- Kwok S., Purton C. R., Fitzgerald P. M., 1978, *ApJ*, 219, L125
- Lane A. P., 1982, PhD thesis, Univ. Massachusetts
- Lawlor T. M., MacDonald J., 2003, *ApJ*, 583, 913
- Le Bertre T., 1988, *ESO Messenger*, 51, 24
- Le Bertre T., 1993, *A&AS*, 97, 729
- Le Bertre T., Nyman L.-A., 1990, *A&A*, 233, 477
- Le Sidaner P., Le Bertre T., 1996, *A&A*, 314, 896
- Lucke P. B., 1978, *A&A*, 64, 367
- Marten H., Szczerba R., 1997, *A&A*, 325, 1132
- Nakashima J., Deguchi S., 2003, *PASJ*, 55, 229
- Nyman L.-A., Hall P. J., Le Bertre T., 1993, *A&A*, 280, 551
- Osterbrock D. E., 1989, *Astrophysics of Gaseous Nebulae*. University Science Books, Mill Valley
- Parker Q. A., Phillipps S., 1998, *A&G*, 39, 10
- Parker Q. A., Phillipps S., 2003, in Ikeuchi S., Hearnshaw J., Hanawa T., eds, *ASP Conf. Ser. Vol. 289, The Proceedings of the IAU 8th Asian-Pacific Regional Meeting, Volume I*. Astron. Soc. Pac., San Francisco, p. 165
- Parker Q. A., Morgan D. H., 2003, *MNRAS*, 341, 961
- Parker Q. A. et al., 2003a, in Dopita M., Kwok S., Sutherland R., eds, *Proc. IAU Symp. 209, Planetary Nebulae and Their Role in the Universe*. Astron. Soc. Pac., San Francisco, p. 25
- Parker Q. A. et al., 2003b, in Dopita M., Kwok S., Sutherland R., eds, *Proc. IAU Symp. 209, Planetary Nebulae and Their Role in the Universe*. Astron. Soc. Pac., San Francisco, p. 41
- Persi P., Ferrari-Toniolo M., Busso M., Origlia L., Robberto M., Scaltriti F., Silvestro G., 1990, *AJ*, 99, 303
- Price S. D., Walker R. G., 1976, *Environmental Research Papers*, Hanscom AFB, Mass. Air Force Geophysics Laboratory, Optical Physics Division
- Reid M. J., Menten K. M., 1997, *ApJ*, 476, 327
- Sevenster M., 2002a, *AJ*, 123, 2772
- Sevenster M., 2002b, *AJ*, 123, 2788
- Sevenster M. N., Chapman J. M., Habing H. J., Killeen N. E. B., Lindqvist M., 1997a, *A&AS*, 122, 79
- Sevenster M. N., Chapman J. M., Habing H. J., Killeen N. E. B., Lindqvist M., 1997b, *A&AS*, 124, 509
- Suh K.-W., 1999, *MNRAS*, 304, 389
- van der Veen W., Habing H., 1988, *A&A*, 194, 125
- van Langevelde H. J., van der Heiden R., van Schooneveld C., 1990, *A&A*, 239, 193
- Vassiliadis E., Wood P. R., 1993, *ApJ*, 413, 641
- Vassiliadis E., Wood P. R., 1994, *ApJS*, 92, 125
- Wainscoat R., Cohen M., Volk K., Walker H. F., Schwartz D. E., 1992, *ApJS*, 83, 111
- Walker H. F., Cohen M., 1988, *AJ*, 95, 1801
- Walker H. F., Cohen M., Volk K., Wainscoat R., Schwartz D. E., 1989, *AJ*, 98, 2163
- Welty A. D., Fix J. D., Mutel R. L., 1987, *ApJ*, 318, 852
- Zijlstra A. A., Te Lintel Hekkert P., Pottasch S. R., Caswell J. L., Ratag M., Habing H. J., 1989, *A&A*, 217, 157
- Zijlstra A. A., Chapman J., Te Lintel Hekkert P., Comeron F., Norris R. P., Molster F. J., Cohen R. J., 2001, *MNRAS*, 322, 280

This paper has been typeset from a $\text{\TeX}/\text{\LaTeX}$ file prepared by the author.